

Antagonistic interactions between benzo[a]pyrene and C₆₀ in toxicological response of Marine Mussels

Audrey Barranger^{1,†,‡}, Laura M. Langan^{1,‡,†}, Graham A. Rance^{2,3}, Yann Aminot⁴, Nicola J. Weston³, Farida Akcha⁵, Michael N. Moore^{1,6,7}, Volker M. Arlt^{8,9}, Vikram Sharma¹, Andrei N. Khlobystov^{2,3}, James W. Readman⁴ and Awadhesh N. Jha^{1,*}

¹ School of Biological and Marine Sciences, University of Plymouth, United Kingdom; audrey.barranger@univ-rennes1.fr, laura.langan@plymouth.ac.uk, vikram.sharma@plymouth.ac.uk, a.jha@plymouth.ac.uk

² School of Chemistry, University of Nottingham, University Park, Nottingham, NG7 2RD, United Kingdom; graham.rance@nottingham.ac.uk, andrei.khlobystov@nottingham.ac.uk

³ Nanoscale and Microscale Research Centre, University of Nottingham, University Park, Nottingham, NG7 2RD, United Kingdom; nicola.weston@nottingham.ac.uk

⁴ Centre for Chemical Sciences, University of Plymouth, Plymouth, United Kingdom; yann.aminot@ifremer.fr, james.readman@plymouth.ac.uk

⁵ Ifremer, Laboratory of Ecotoxicology, Nantes, France; farida.akcha@ifremer.fr

⁶ Plymouth Marine Laboratory, Prospect Place, The Hoe, Plymouth, United Kingdom; mnm@pml.ac.uk

⁷ European Centre for Environment & Human Health (ECEHH), University of Exeter Medical School, Knowledge Spa, Royal Cornwall Hospital, Truro, Cornwall, United Kingdom

⁸ Analytical and Environmental Sciences Division, King's College London, MRC-PHE Centre for Environmental & Health, London, United Kingdom; volker.arlt@kcl.ac.uk

⁹ NIHR Health Protection Research Unit in Health Impact of Environmental Hazards at King's College London in partnership with Public Health England, London, United Kingdom

* Correspondence: a.jha@plymouth.ac.uk; Tel.: +44 1752 584633

‡ Present Address: Université de Rennes 1 / Centre National de la Recherche Scientifique, UMR 6553 ECOBIO, Rennes, F-35000, France

Present Address: Department of Environmental Science, Baylor University, Waco, Texas, USA

† These authors contributed equally to this work.

S1. Characterisation of fullerenes in seawater

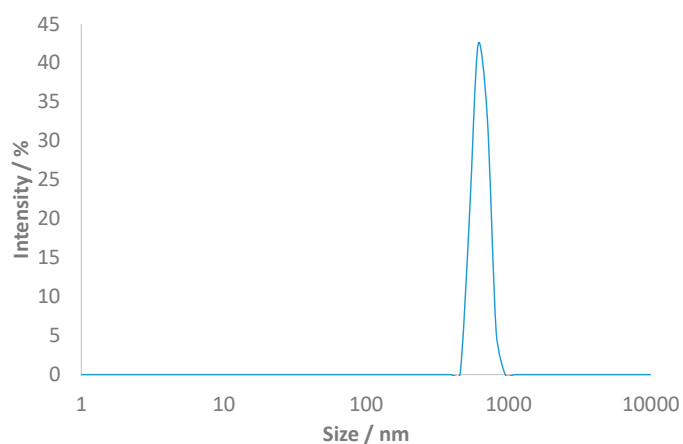


Figure S1. Representative particle size distribution showing the intensity-weighted hydrodynamic diameter (d_H) of nC_{60} in mussel-exposed seawater as determined by DLS (653 ± 87 nm). The maximum concentration of nC_{60} in seawater 0.1 mg mL^{-1} , which is significantly higher than that utilised in exposure experiments, but within the range detectable by the instrument. Control measurements of seawater in the absence of nC_{60} yielded no measurable scatterers.

Table S1. The influence of benzo(a)pyrene (B[a]P) of the hydrodynamic diameter (d_H) of nC_{60} in mussel-exposed seawater as determined by DLS. The addition of B[a]P results in a subtle decrease in the mean size of aggregates; however, the decrease is small and likely insignificant given the broad range of sizes observed within the respective size distributions.

[B[a]P] / $\mu\text{g/L}$	d_H / nm
0	653 ± 87
5	601 ± 62
50	555 ± 64
100	543 ± 55

S2. Concentration of B[a]P and C₆₀ in seawater

Table S2. The concentration of B[a]P in seawater at T0, day 1 and day 3. Data are means SE (n = 3)

Treatments	BaP concentration ($\mu\text{g L}^{-1}$)		
	T0	Day 1	Day 3
Solvent control	< 0.25	< 0.25	< 0.25
BaP 5 $\mu\text{g L}^{-1}$	4.8 \pm 1.8	1.3 \pm 2.0	0.1 \pm 0.1
BaP 50 $\mu\text{g L}^{-1}$	52.9 \pm 7.3	7.3 \pm 4.1	0.7 \pm 0.4
BaP 100 $\mu\text{g L}^{-1}$	94.4 \pm 23.4	6.1 \pm 4.9	1.5 \pm 1.2
C ₆₀ + BaP 5 $\mu\text{g L}^{-1}$	6.2 \pm 1.2	0.9 \pm 0.9	0.1 \pm 0.1
C ₆₀ + BaP 50 $\mu\text{g L}^{-1}$	52.0 \pm 15.8	5.1 \pm 6.7	1.3 \pm 1.5
C ₆₀ + BaP 100 $\mu\text{g L}^{-1}$	102.0 \pm 21.5	15.4 \pm 16.0	2.5 \pm 1.6

Table S3. The concentration of nC₆₀ in seawater at T0, day 1 and day 3. Data are means SE (n = 3).

Treatments	C ₆₀ concentration ($\mu\text{g L}^{-1}$)		
	T0	Day 1	Day 3
Solvent control	< 0.2	< 0.2	< 0.2
C ₆₀ 0.01 mg L ⁻¹	7.3 \pm 1.8	< 0.2	< 0.2
C ₆₀ 0.1 mg L ⁻¹	63.8 \pm 11.9	0.4 \pm 0.6	< 0.2
C ₆₀ 1 mg L ⁻¹	427.6 \pm 45.3	0.5 \pm 0.5	< 0.2
C ₆₀ + BaP 5 $\mu\text{g L}^{-1}$	518.3 \pm 48.6	0.9 \pm 0.6	0.5 \pm 0.7
C ₆₀ + BaP 50 $\mu\text{g L}^{-1}$	477.5 \pm 107.9	2.5 \pm 4.3	< 0.2
C ₆₀ + BaP 100 $\mu\text{g L}^{-1}$	604.1 \pm 52.0	2.7 \pm 3.9	< 0.2

S3. Transmission electron microscopy analysis of labelled fullerenes

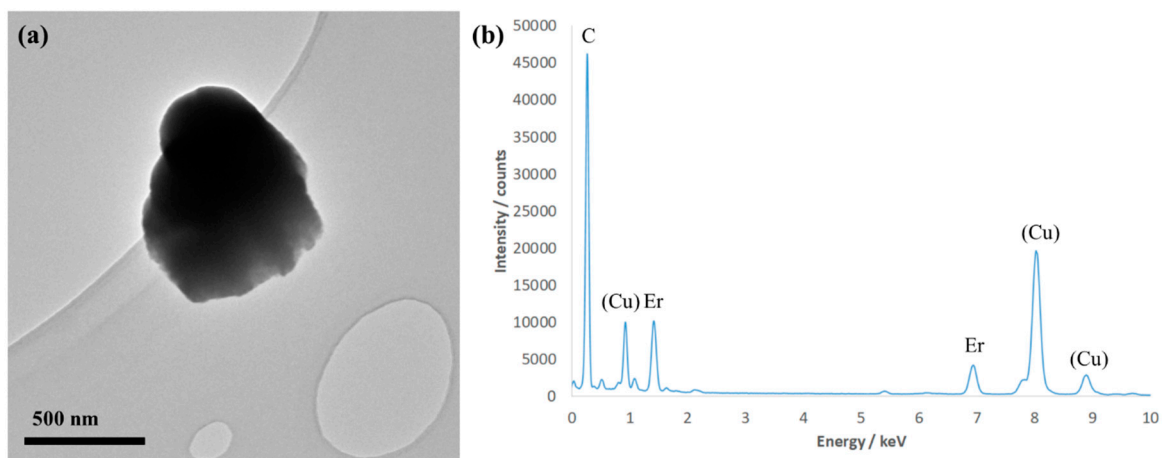


Figure S2. (a) Bright-field TEM and (b) point EDX spectroscopy analysis of $\text{Er}_3\text{N}@\text{C}_{80}$. The dark features (which comprise high atomic number elements) in the bright-field TEM images are used to visually locate nanoscale species of interest. This analysis confirms (i) the formation of $n(\text{Er}_3\text{N}@\text{C}_{80})$ aggregates, analogous to those observed for $n\text{C}_{60}$ from light scattering measurements and (ii) the presence of Er from the characteristic M and $\text{L}\alpha$ lines at 6.95 and 1.41 eV, respectively. The presence of Cu, plus trace quantities of Cr and Au, in the EDX spectrum is associated with the TEM grid and column assembly.

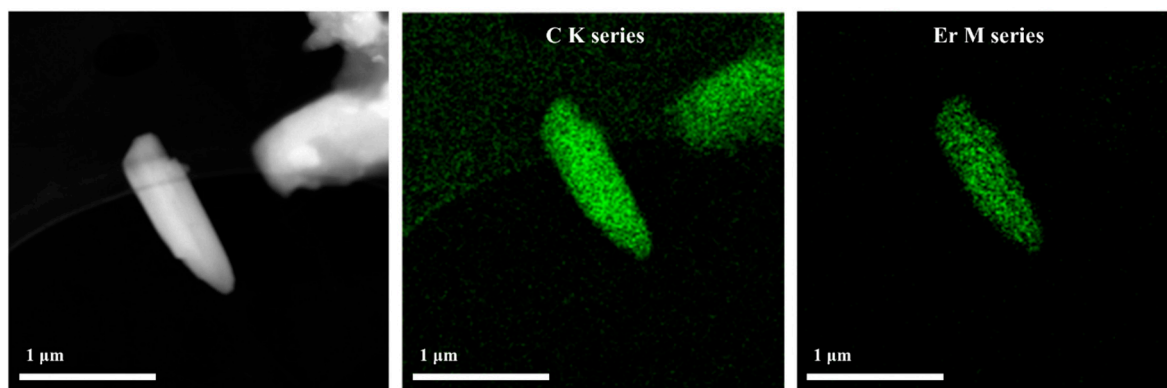


Figure S3. Dark-field STEM and EDX spectroscopy mapping analysis of $\text{Er}_3\text{N}@\text{C}_{80}$, confirming the necessity for spectroscopy to confirm the presence of labelled fullerenes, using the characteristic X-rays emitted from Er upon electron irradiation.

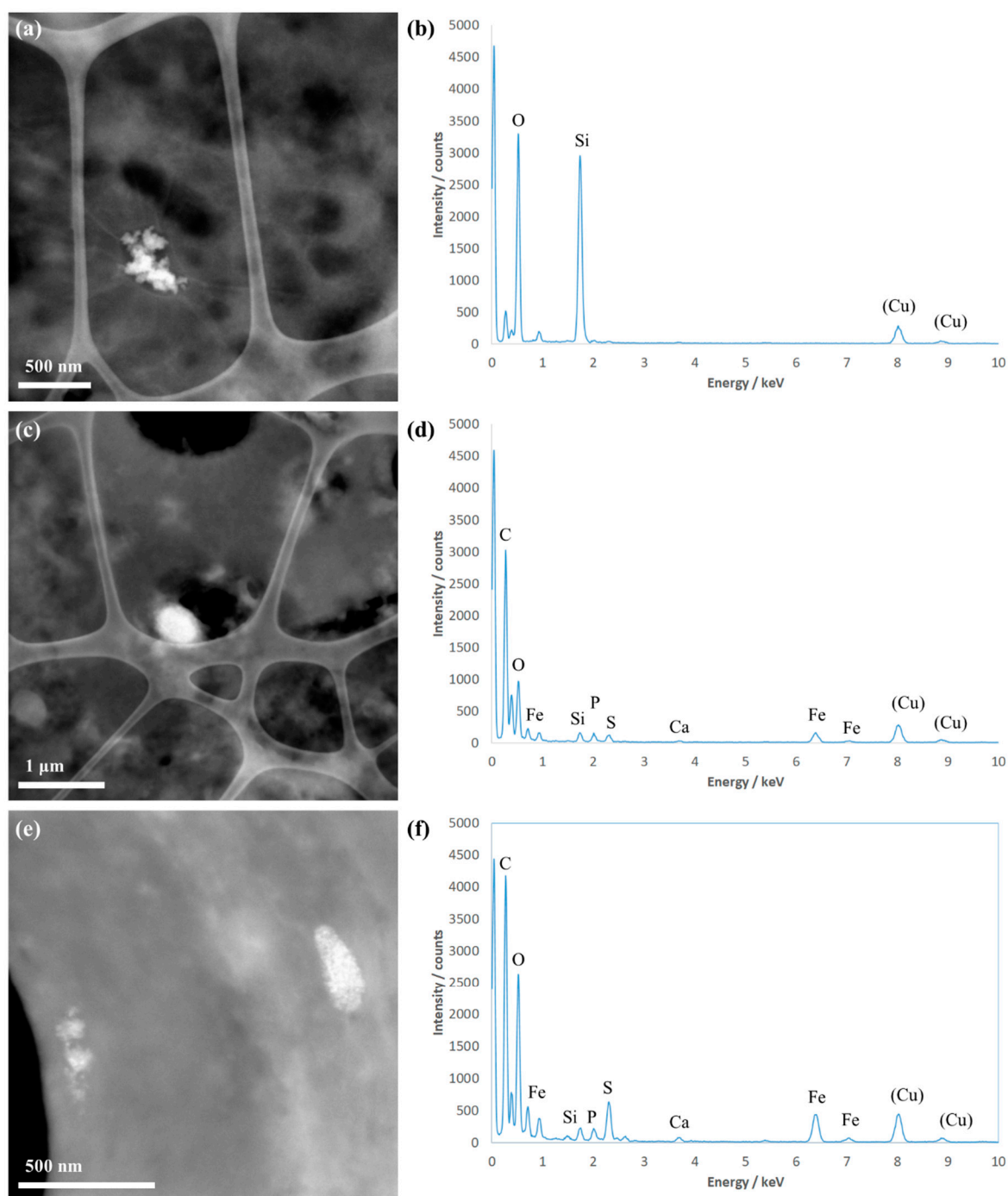


Figure S4. (a,c,e) Dark-field STEM and (b,d,f) corresponding point EDX spectroscopy analysis of cross-sections of mussel digestive gland exposed to $\text{Er}_3\text{N@C}_{80}$. The bright features (which comprise high atomic number elements) in the dark-field STEM images are used to visually locate nanoscale species of interest. The EDX spectra collected from these explicit locations confirm the presence of silica (b) and iron (d and f) as typical environmental contaminants, but no evidence for the uptake of labelled fullerene aggregates was directly observed. However, the presence of labelled fullerenes within the mussel digestive gland was confirmed by whole tissue ICP-MS analysis and therefore the absence of evidence from our STEM-EDX investigations implies that the labelled fullerenes are dispersed at potentially the near single molecule level, below the level of identification by imaging or sensitivity of *in situ* spectroscopy. The presence of Cu in the EDX spectra is associated with the specimen grid and instrument column assembly.